

The Phase Composition of Electric Furnace Slag

Štefica Cerjan-Stefanović,^a Alenka Rastovčan-Mioč,^b
and Vjera Novosel-Radović^c

^a Department of Analytical Chemistry, Faculty of Chemical Engineering and Technology, University of Zagreb, Marulićev trg 19, HR-10000 Zagreb, Croatia

^b Department of Materials, Faculty of Metallurgy, University of Zagreb, Aleja narodnih heroja 3, HR-44000 Sisak, Croatia

^c Institute for Development and Research, Željezara Sisak, Otokara Keršovanija 2, HR-44000 Sisak, Croatia

Received May 31, 1995; revised December 21, 1995; accepted February 1, 1996

Elementary and phase composition as well as micrography of the electric furnace slag were examined. The base of slag is made from phases containing Fe, Mn and Ca. Grains differ in size and shape, they cling together to form bigger or smaller agglomerates, depending on separated fractions. Relative distribution of identified phases in separated fractions is presented and the possibility of phase separation by means of successive fragmentation and sieve analysis was noticed. The slag defined in that way could find application in cement production and construction industry. The electric furnace slag deposits which pollute the water and ground as well as disfigure the environment can thus be reduced.

INTRODUCTION

Steel is a solid solution of carbon, manganese, silicon, chromium and a number of other elements, e.g. nickel, tungsten, molybdenum and vanadium in iron. Depending on the requirements which steel is supposed to meet, larger or smaller quantities of elements are included in its composition. In this way, the mechanical and physical properties of steel are improved and emergence of various defects is prevented.

Steel always contains certain amounts of harmful substances: phosphorus, sulphur, oxygen, hydrogen and nitrogen. Such admixtures enter steel in the melting process either from the charge material or from the surrounding atmosphere. In order to remove the admixtures, melting is regulated in such a way that first the oxidation, and then the deoxidation processes are carried out. The oxidation process refers to oxidation of admixtures found in the metal charge. If the process is carried out in the basic furnace, phosphorus and a certain amount of sulphur are carried over into slag, in its course. Oxidation is mostly performed with addition of iron ore. When oxidation is completed, the slag is poured off to prevent slag phosphorus to reenter the metal during the deoxidation process. Mixtures of ground coke and lime, ferrosilicon and lime, etc. are used in the deoxidation process in order to completely remove the sulphur. Slag liquidity is increased with addition of fluorspars. Besides removing harmful admixtures from the liquid metal, the importance of slag is in its acceptance of the valid alloy additive and in steel protection.¹⁻⁴

(Details about carbon and Hadfield steel making as well as about the accompanying slag discussed in this paper, see in references⁵⁻⁸).

Considerable quantities of slag demand a special approach to deposition, storing and taking care of such material, which can pollute the air, water and soil as well as disfigure the environment. Previous examination showed a balanced chemical composition of slag, a low content of radionuclides and toxic metals.⁹ The use of blast and electric furnace slag in cement production was also discussed.¹⁰⁻¹¹ It was observed that the applicability of slag depends on its elementary and phase composition. Now, the composition and micrography as well as separation of phase components by means of successive fragmentation or sieve analysis are reported.

EXPERIMENTAL

Sampling

To define the elementary and the phase composition as well as the micrography of slag, four characteristic samples of electric furnace slag were used. The samples were taken during the casting process of 0.545 low carbon steel and Hadfield steel. They were marked with numbers 1 to 4. Samples 1 and 2 are slag of the same origin, of the same steel grade, 0.545 low carbon steel, and from the same charge. They differ only in the temperature at which they were taken: sample 1 was taken at 1833 K, and sample 2 at 1903 K. Samples 3 and 4 are slag produced in the casting process of the same steel grade (Hadfield steel, same charge), and they also differ in the temperature at which they were taken: sample 3 was taken at 1883 K, and sample 4 at 1763 K. Samples 1-4 were taken with a spoon on a plate and cooled with water. Cold samples (294 K) were ground and homogenized for 150 minutes in a »Herzog« vibration mill. Successive quartering and crushing provided 100 g of each sample (average samples).

The average samples 1–4 obtained in this way were characterized by means of:

- chemical analysis,
- X-ray emission spectrometry,
- X-ray powder diffraction and
- scanning electron analysis.

However, in order to be able to compare the grain size and the mineralogical composition of slag, it was necessary to prepare the samples for specific analyses in a different way. The cooled samples 1 and 3 were crushed in a vibration mill for 10 minutes. Such samples were separated by means of sieve analysis and characterized by means of:

- X-ray powder diffraction and
- scanning electron analysis.

Slag Characterization

The chemical composition of average slag samples was investigated by means of a traditional chemical analysis.¹² Sulphur content was determined by the burning down procedure using the »Leco« automatic analyzer for sulphur and carbon C,S-444.

For the analysis by X-ray emission spectrometry, average slag samples were preliminarily prepared by being pressed over a boric acid backing pallet. The briquettes were measured on a Philips 1410/10 sequential semi-automatic X-ray spectrometer (Au tube target, 50 kV, and 20 mA, using analyzer crystal ADP (101), and gas flow counter).

By means of sieve analysis (according to DIN), five fractions were separated in samples 1 and 3: > 630 μm , 125–630 μm , 90–125 μm , 50–90 μm and < 50 μm and they have been ground for 10 minutes.

For the X-ray powder diffraction analysis, all of the samples (average samples 1, 2, 3 and 4 and by sieve analysis separated fractions in samples 1 and 3, which had been ground for 10 minutes) were subsequently ground and homogenized in a Spex Mixer Mill tungsten-carbide grinding container for 10 minutes.

All X-ray diffraction powder patterns were collected at room temperature using a Philips counter diffractometer with monochromatized (graphite monochromator) $\text{CoK}\alpha$ ($\lambda = 1.790 \text{ \AA}$) radiation.

For scanning electron microscopy, samples were attached to a support with colloidal silver and coated with an evaporated layer of copper in a JEOL type evaporator. Electron micrographs were taken on the JEOL JXA 50A scanning electron microscope.

RESULTS AND DISCUSSION

Results of qualitative analysis of electric furnace slag by X-ray emission spectrometry are shown in Table I. The recorded X-ray spectra (range 10 to $55^\circ 2\theta$) of analyzed samples are given in Figure 1. In Figure 1 peaks $\text{SiK}\alpha$ ($84^\circ 2\theta$) and $\text{MgK}\alpha$ ($136.47^\circ 2\theta$) are not visible. The peaks were considered by X-ray spectrometer tables.¹³ Each element was considered as major, mi-

TABLE I
Elementary composition of electric furnace slag

Sample	Identified elements															
	Fe	Cr	Mn	Ca	Cu	Zn	Si	Ba	V	Co	Mo	Mg	Ti	Al	Sb	K
1	+	+	+	+	+	+	+	+	+	+	+	+	+	+	+	+
2	+	+	+	+	+	+	+	+	+	-	+	+	+	+	+	+
3	+	+	+	+	+	+	+	-	+	-	+	+	+	-	-	+
4	+	+	+	+	+	+	+	-	+	-	-	+	+	-	-	+

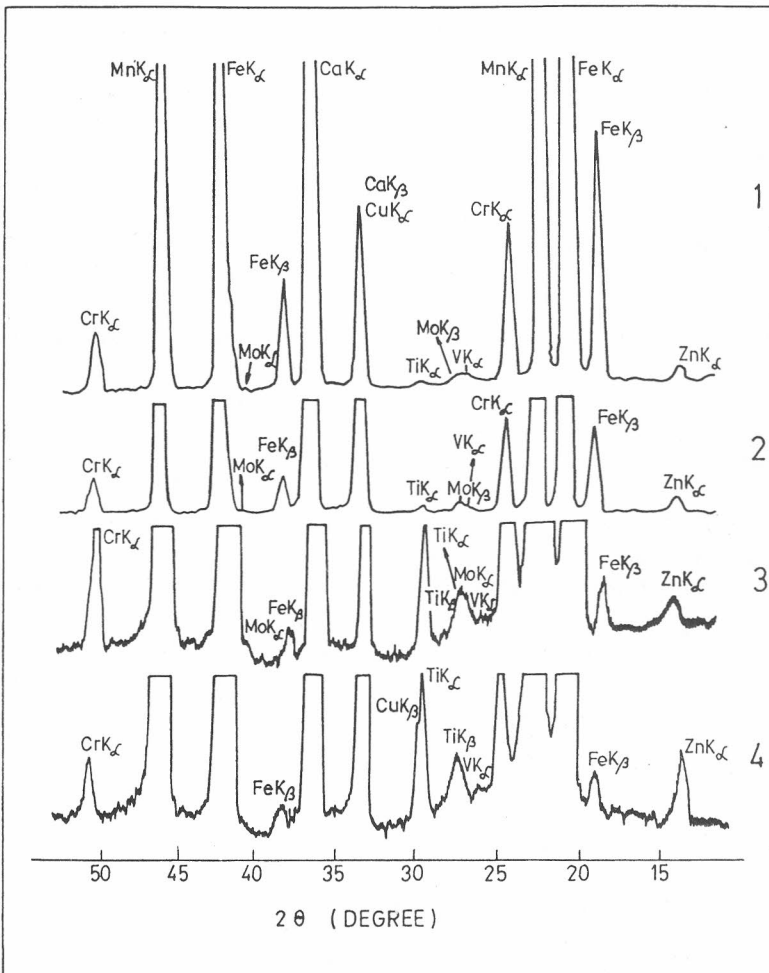


Figure 1. X-ray spectrum of electric furnace slag samples.

TABLE II
Mass fractions /% of electric furnace slag

Sample number	SiO ₂	Fe ₂ O ₃	FeO	CaO	MgO	Mn ₂ O ₃	Al ₂ O ₃	P ₂ O ₅	S	K ₂ O	Na ₂ O
1	33.22	9.10	8.35	20.97	10.70	14.22	3.23	0.034	0.010	0.65	0.27
2	28.66	0.43	6.77	26.49	23.40	9.48	4.56	0.022	0.018	0.62	0.20
3	31.06	2.07	0.00	12.69	16.69	36.51	0.00	0.050	0.010	0.76	0.28
4	31.74	2.40	0.00	12.70	18.64	33.66	0.00	0.048	0.010	0.68	0.24

nor or trace constituent on the basis of the intensity of its peak.¹⁴ The results of the quantitative chemical analysis are shown in Table II. Minor deviations in the chemical composition of the tested slag as compared to reference figures are the result of the higher charge quality.^{3,8}

In sample 1 Si, Ca, Fe and Mn were identified as major constituents, Mg, Al, Cr and Cu as minor constituents, and Zn, V, Mo, K, Ti, Ba, Sb and Co as traces. In sample 2 Si, Mg and Ca were identified as major constituents, Fe, Mn, Cr, Al and Cu as minor constituents, and Zn, Ti, K, Mo, V, Sb and Ba as traces. In samples 3 and 4 Si, Ca, Mg and Mn were identified as major constituents, Fe, Ti, Cr and Cu as minor constituents, and Zn, K and V as traces. In sample 3 there was Mo, too identified as trace constituent.

According to these results, a difference was noticed in the elemental concentration of analyzed samples. Thus, sample 1 contained more Fe, Mn, Cr, Si and V than sample 2. This sample contained more Ca and Cu, whereas the concentration of Zn and Mo was almost the same.

The electric furnace slag sample 3 contained slightly more Mn in comparison to sample 4.

The results of X-ray diffraction phase analysis of average samples of furnace slag are given in Figures 2 and 3. All the observed phases except CaOFe₂O₃, α CaOSiO₂ and MgSiO₃, were identified according to the JCPDS-PDF card number: 1-1127, 4-0326, 5-0528, 5-0657, 8-458, 9-151, 10-319, 11-353, 11-480, 12-145, 12-284, 12-432, 12-434, 13-342, 13-343, 14-77, 14-376 and 14-644.

Other phases were identified according to Narita.¹⁵ The obtained results of the X-ray diffraction phase analysis confirm the conclusions about the phase composition of electric furnace slag samples derived from the results of elementary and quantitative analyses. The basis of electric furnace slag in samples 1 and 2 is made of a mixture of calcium-ferrite phases: CaOFe₂O₃, CaO2Fe₂O₃, 4CaO7Fe₂O₃ and calcium-manganese silicates (Ca,Mn)₂SiO₄ and CaOMgOSiO₂. Other identified phases: CaCrO₄ and α CaCr₂O₄, CuMn₂O₄, CuCr₂O₄ and α CaOSiO₂ as compared to the basic

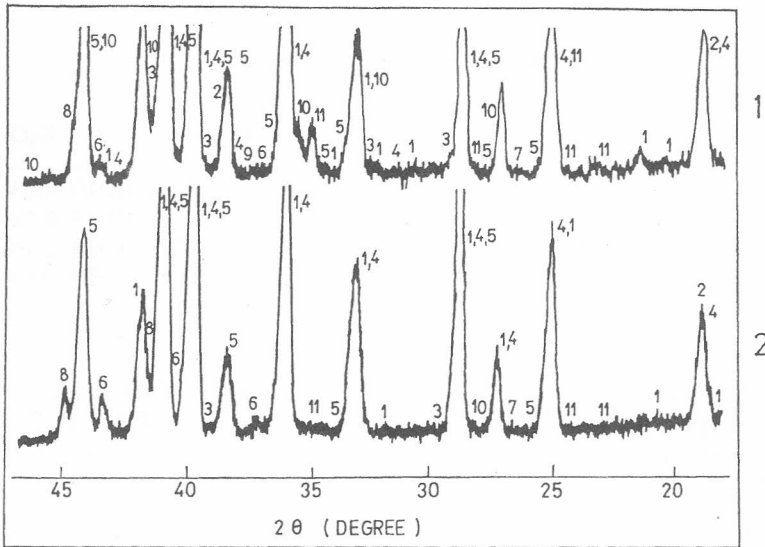


Figure 2. X-ray diffraction patterns of average electric furnace slag samples 1 and 2. Identified phases: 1 – mixture of $\text{CaO}\cdot\text{Fe}_2\text{O}_3$, $\text{CaO}\cdot 2\text{Fe}_2\text{O}_3$, α and β $4\text{CaO}\cdot 7\text{Fe}_2\text{O}_3$; 2 – $\alpha\text{CaCr}_2\text{O}_4$; 3 – CaCrO_4 ; 4 – $(\text{Ca},\text{Mn})_2\cdot\text{SiO}_4$; 5 – $\text{CaO}\cdot\text{MgO}\cdot\text{SiO}_2$; 6 – CuMn_2O_4 ; 7 – γMnO_2 ; 8 – CuCr_2O_4 ; 9 – $\alpha\text{CaO}\cdot\text{SiO}_2$; 10 – $\text{CaO}\cdot\text{Al}_2\text{O}_3\cdot 2\text{SiO}_2$; 11 – phase of not determined composition.

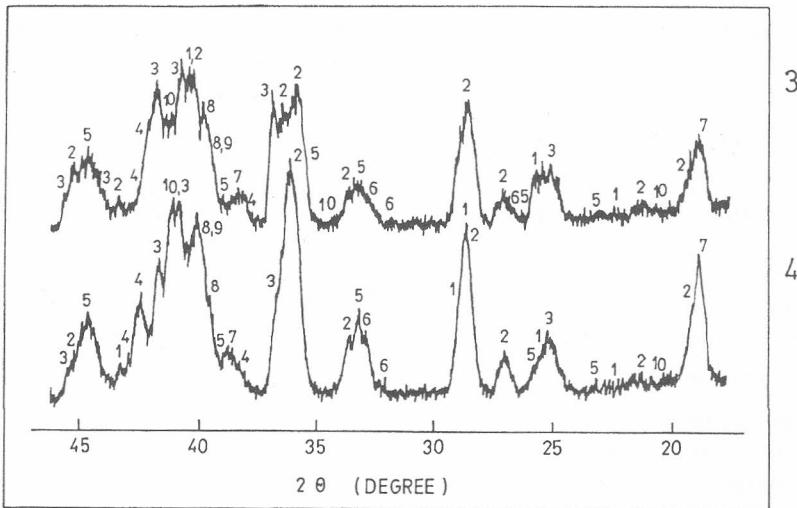
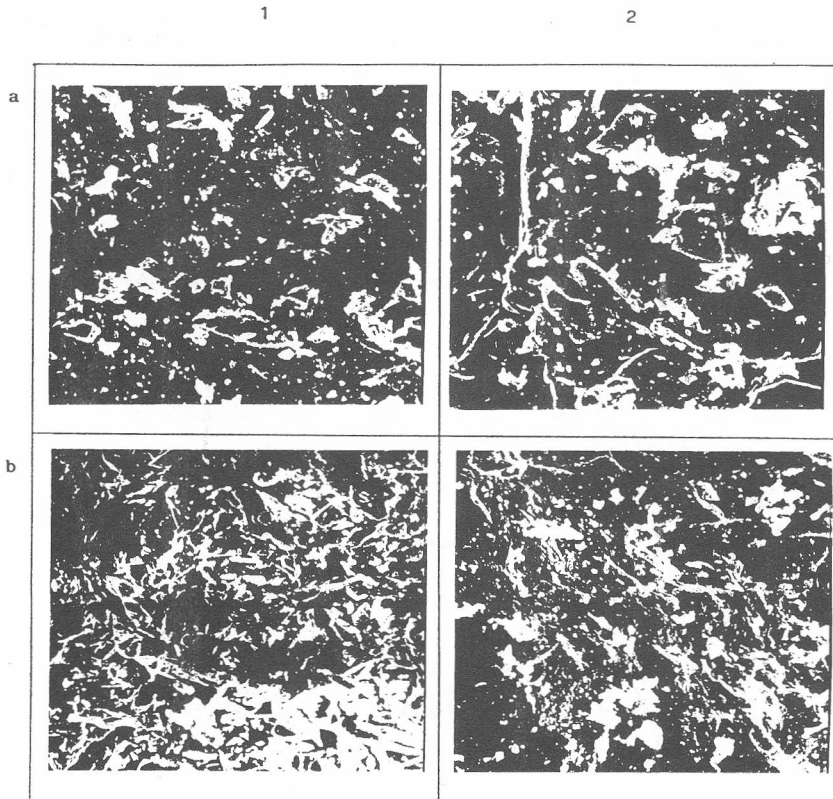


Figure 3. X-ray diffraction patterns of average electric furnace slag samples 3 and 4. Identified phases: 1 – MnO ; 2 – $\text{MnO}\cdot\text{SiO}_2$; 3 – $(\text{Mn},\text{Mg})_2\cdot\text{SiO}_4$; 4 – Mn_3O_4 ; 5 – $3\text{CaO}\cdot 2\text{SiO}_2$; 6 – MgSiO_3 ; 7 – $\alpha\text{CaO}\cdot\text{SiO}_2$; 8 – $\text{CaO}\cdot 2\text{Fe}_2\text{O}_3$; 9 – $2\text{FeO}\cdot\text{SiO}_2$; 10 – MnFe_2O_4 .

phases are found in a smaller or considerably smaller concentration, such as for example γMnO_2 , $\text{CaOAl}_2\text{O}_3\text{2SiO}_2$, and sodium aluminium silicates of not determined composition. As opposed to that, in sample 3 and 4 the slag basis is made of phases MnO , MnOSiO_2 and 3CaO2SiO_2 which is in agreement with the reference figures.^{8,16,17}

From the obtained X-ray diffraction patterns of average electric furnace slags (Figures 2 and 3) it is also evident that the X-ray diffraction lines vary greatly in sharpness, especially in samples 3 and 4.

According to Klug and Alexander¹⁸ this phenomenon was the result of different sharpness and grain size and their distribution. These observations are confirmed by the results of scanning electron microscopy (Figure 4).



53 μm

Figure 4. Scanning electron micrographs of average electric furnace slag sample 1 (1a), 2 (1b), 3 (2a) and 4 (2b). Enlargement: 500 \times .

This is confirmed by the results of the X-ray diffraction analysis of electric furnace slag samples 1 and 3 separated by sieve analysis. Namely, the already obtained X-ray diffraction patterns of fraction from $> 630 \mu\text{m}$ to $50 \mu\text{m}$, separated from electric furnace slag, differ from the X-ray diffraction patterns of average samples (Figures 5 and 6). This difference can be observed in the intensity and profile of X-ray diffraction lines and in their recorded number. According to the phase analysis results in separated fractions of sample 1, they correspond to the following phases: CaOFe_2O_3 , $\text{CaO}_2\text{Fe}_2\text{O}_3$, and

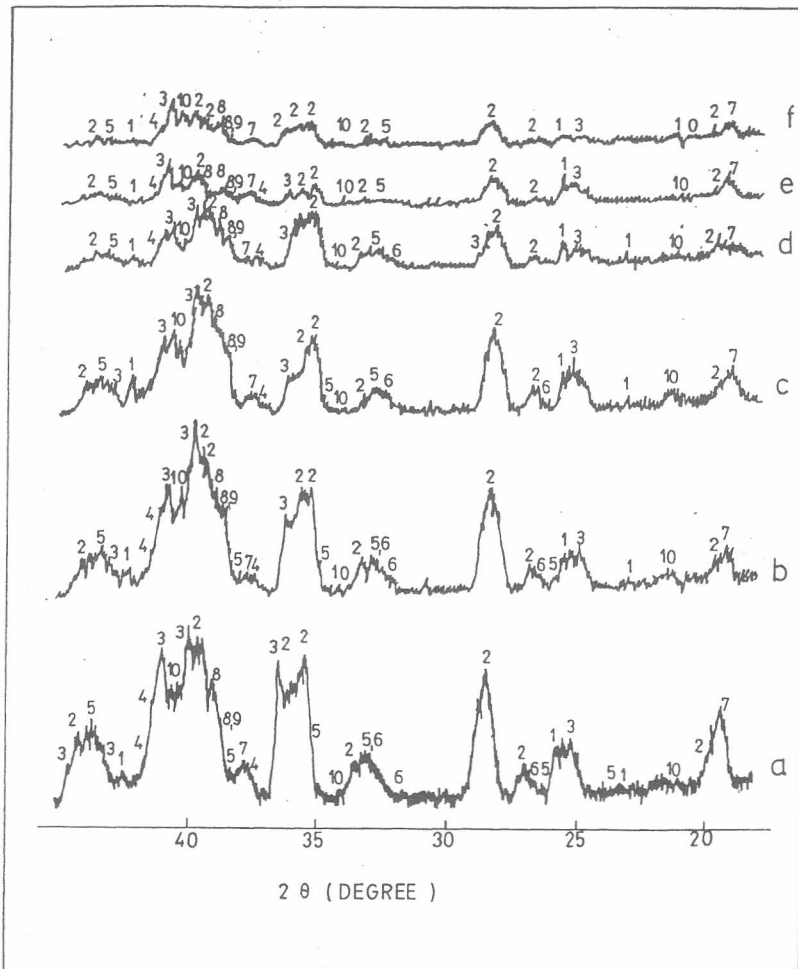


Figure 6. X-ray diffraction patterns of the fractions: b - $< 50 \mu\text{m}$, c - $50-90 \mu\text{m}$, d - $90-125 \mu\text{m}$, e - $125-630 \mu\text{m}$ and f - $> 630 \mu\text{m}$ separated from a - electric furnace slag sample 3.

$4\text{CaO} \cdot 7\text{Fe}_2\text{O}_3$, CaCrO_4 , $\alpha\text{CaCr}_2\text{O}_4$, $(\text{Ca},\text{Mn})_2\text{SiO}_4$, CaOMgOSiO_2 , CuMnO_2 , γMnO_2 , CuCr_2O_4 and αCaOSiO_2 , $\text{CaOAl}_2\text{O}_3 \cdot 2\text{SiO}_2$, and Na-Al-Si with not determined formula (Figure 5), and in sample 3: MnO , MnOSiO_2 , $(\text{Mn},\text{Mg})_2\text{SiO}_4$, MnFe_2O_4 , $3\text{CaO} \cdot 2\text{SiO}_2$, MgSiO_3 , αCaOSiO_2 , $\text{CaO} \cdot 2\text{Fe}_2\text{O}_3$, 2FeOSiO_2 and Mn_3O_4 (Figure 6). Among these phases, only the CaCrO_4 phase was identified in the fraction from 125 to $< 50 \mu\text{m}$.

The observed relative intensities of characteristic reflection 111 $\text{CaO} \cdot 2\text{Fe}_2\text{O}_3$, 100 $\alpha\text{CaCr}_2\text{O}_4$, 222 $(\text{Ca},\text{Mn})_2\text{SiO}_4$, 021 $\text{CaOAl}_2\text{O}_3 \cdot 2\text{SiO}_2$ in separated fractions of slag sample 1 (Figure 7) and 102 MnOSiO_2 , 130 $(\text{Mn},\text{Mg})_2\text{SiO}_4$, 020 MnO , 111 MnFe_2O_4 and 312 $3\text{CaO} \cdot 2\text{SiO}_2$ in separated fractions of slag sample 3 (Figure 8) point to the change. Only in the case of reflection 102

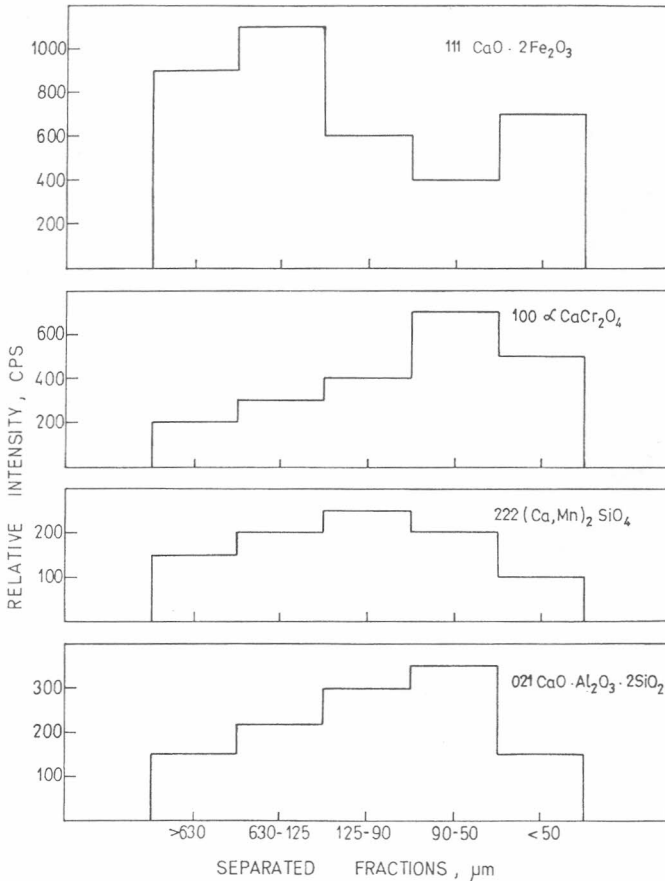


Figure 7. Relative intensity of characteristic reflection of phases in separated fractions of electric furnace slag sample 1.

MnOSiO_2 , the relative intensity decreased with the size of the separated fraction. The relative reflection intensity of other phases shows the maximum value only in one or more separated fractions of samples 1 and 3. Thus in sample 1, the reflex intensity 111 $\text{CaO}2\text{Fe}_2\text{O}_3$ has maximum value in the separated fraction from 630 to 125 μm , 222 $(\text{Ca},\text{Mn})_2\text{SiO}_4$, from 125 to 90 μm , 100 $\alpha\text{CaCr}_2\text{O}_4$ and 021 $\text{CaOAl}_2\text{O}_32\text{SiO}_2$ from 90 to < 50 μm (Figure 7). In separated fractions of sample 3 (Figure 8), the changes of relative reflection intensity 130 $(\text{Mn},\text{Mg})_2\text{SiO}_4$, 020 MnO , 111 MnFe_2O_4 and 312 $3\text{CaO} \cdot 2\text{SiO}_2$ are more expressive.

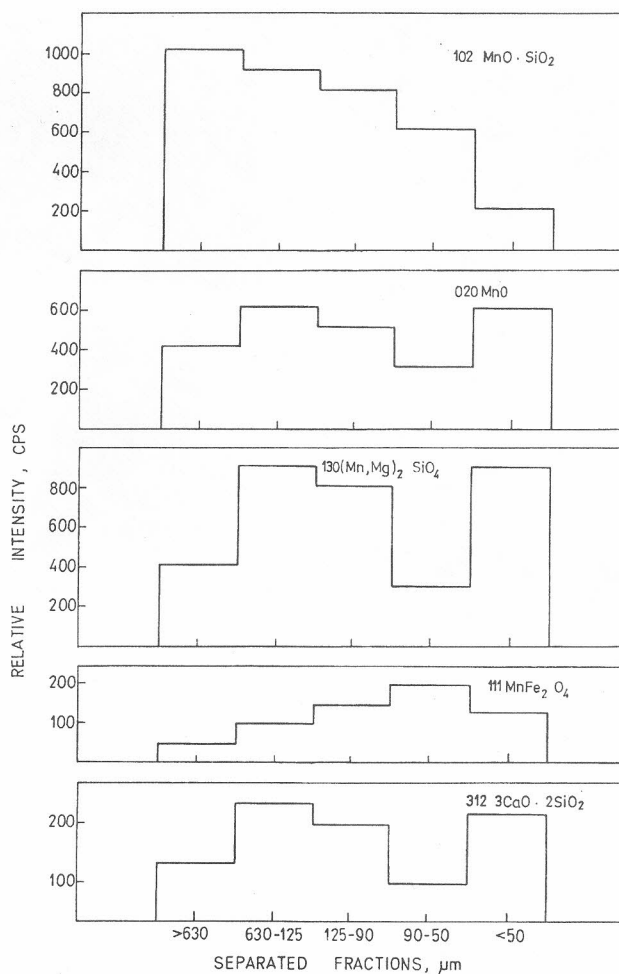


Figure 8. Relative intensity of characteristic reflection of phases in separated fractions of electric furnace slag sample 3.

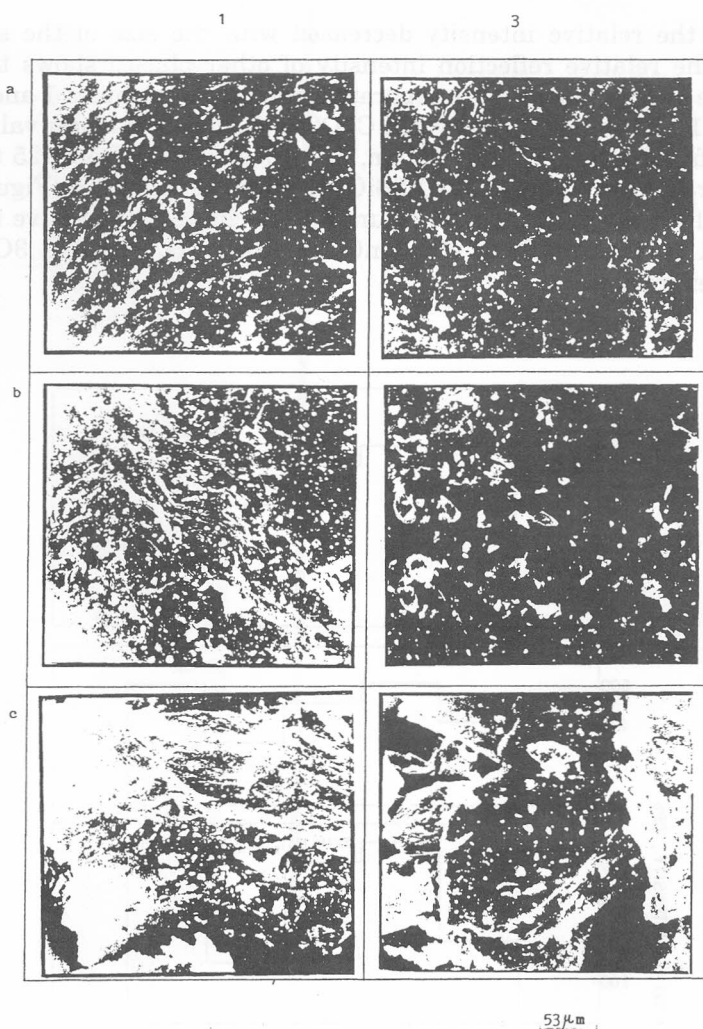


Figure 9. Scanning electron micrographs of fractions: a – $>630 \mu\text{m}$, b – $125\text{--}630 \mu\text{m}$ and c – $90\text{--}125 \mu\text{m}$ separated from 1 – electric furnace slag sample 1 and 3 – electric furnace slag sample 3 (ground and homogenized in a vibration mill for 10 minutes). Enlargement: $500\times$.

Physical properties of the identified phases could effect the reduction rate of grain size hardness, which is of special importance. For example, the hardness of some identified phases is rather different: 7500 N/mm^2 – MnOSiO_2 , 4000 N/mm^2 – MnO^{20} , $10\,000 \text{ N/mm}^2$ – MgSiO_3 , $10\,000 \text{ N/mm}^2$ – αCaOSiO_2 .²¹ It influences the grain distribution of a particular fraction.²² The results of scanning electron microscopy (Figure 9) show agglomeration of grain (espe-

cially of large grains with very small ones) and adhesion of smaller grains to the surface of larger ones. Considering similar phenomena, De Joungh²³ and Hlavay²⁴ described the ability of particle formation.

CONCLUSION

Separated slag fractions differ in size, shape and distribution of phases. Phase separation is possible by means of successive fragmentation. This procedure could enable the use of slag.

REFERENCES

1. J. Lamut and V. Gontarev, International Scientific Conference on the Occasion of the 35th Anniversary of the Department of Ferrous and Foundry Metallurgy, Metallurgical Faculty Košice, Slovakia 1994, Proceedings, p. 560–567.
2. D. C. Hilty, R. W. Farley and D. J. Girardi, Electric Furnace-Steel making, vol. 2, Interscience Publishers, New York 1963.
3. A. D. Kramarov, Proizvodstvo stali v elektropečah, Metallurgija, Moskva 1964.
4. M. B. Hocking, Modern Chemical Technology and Emission Control, Springer Verlag, Berlin 1985.
5. F. P. Edneral, Electrometallurgy of Steel and Ferro-alloys, vol.1, Mir, Moscow 1979.
6. C. E. Sims (ed.), Electric Furnace Steel Making, vol.1, Interscience Publishers, New York 1962.
7. J. Lamut, V. Gontarev, and K. Koch, 4th International Conference of Molten Slag and Fluxed, Sendai, Japan, 1992, Proceedings, p. 481–486.
8. M. J. Gasik (ed.), Metalurgija visokomangancevoj stali, Tehnika, Kijev 1990.
9. A. Rastovčan, Š. Cerjan-Stefanović, V. Novosel-Radović, and J. Kovač, XIV Meeting of Croatian Chemists, Zagreb, 1995, Abstracts, p. 391.
10. Š. Cerjan-Stefanović, V. Novosel-Radović, and A. Rastovčan, *Metalurgija* **33** (1994) 109–112.
11. Š. Cerjan-Stefanović, A. Rastovčan, and R. Rosković, XVI Symposium on Technological Achievements and Ecological Solutions in Cement Production and Cement-Fiber Products, Split, 1995, Proceedings, p. 57–64.
12. EN 196 TEIL 2 (UDC: 666.94:691.54:620.1)
13. X-ray Emission Line Wavelength and Two Theta Tables, ASTM DATA, Series DS 37, Alfa, New Jersey 1965.
14. E. P. Bertin, Principles and Practice of X-ray Spectrometric Analysis, Plenum Press, New York, 1970, p. 287–302.
15. K. Narita, Kristaličeskaja struktura nemetaličeskikh vključenij v stali, Metalurgija, Moskva, 1966, p. 50, 59 and 116.
16. Atlas Šlakov, Metalurgija, Moskva 1985.
17. L. Tadić, Mišljenje o eventualnom utjecaju na okolinu objekta za preradu i odlaganje čeličanske troske, Metalurški fakultet, Sisak, 1986. (in Croatian)
18. H. P. Klug and L. E. Alexander, X-Ray Diffraction Procedures for Polycrystalline and Amorphous Materials, J. Wiley and Sons, New York 1962, p. 491–532.

19. V. Novosel-Radović, Da. Maljković, *X-ray Spectrometry* **16** (1987) 211–215.
20. R. Kiessling, M. Lange, *Non Metallic Inclusions in Steel, Part I*, Iron and Steel Institute, London, 1964, p. 26 and 44.
21. R. Kiessling, M. Lange, *Non Metallic Inclusions in Steel, Part II*, Iron and Steel Institute, London, 1966, p. 17 and 51.
22. V. Novosel-Radović, T. Sofilić, and Da. Maljković, *Metalurgija* **34** (1995) 13–17.
23. N. K. De Joungh, *Analytical Bulletin Philips*, 79.177/FS 25, May 1970, Philips Eindhoven.
24. J. Hlavay and J. Inczedy, *Kem. Kozl.* **50** (1978) 447–456; *Chem. Abstr.* **90** (1979) 153929t.

SAŽETAK

Fazni sastav elektropećne troske

Štefica Cerjan-Stefanović, Alenka Rastovčan-Mioč i Vjera Novosel-Radović

Ispitani su elementarni i fazni sastav, te mikrografija elektropećne troske. Osnovu troske čine faze koje sadrže Fe, Mn i Ca. Zrna su različite veličine i oblika, međusobno slijepljena u veće ili manje aglomerate, ovisno o izdvojenim frakcijama. Prikazana je relativna raspodjela identificiranih faza u separiranim frakcijama i uočena je mogućnost separacije faza uz pomoć sukcesivne fragmentacije i sitene analize. Tako definirana troska mogla bi naći primjenu u proizvodnji cementa i graditeljstvu. Na taj način smanjuje se deponij elektropećne troske koji onečišćuje vodu i tlo, te nagrđuje okoliš.